DEVELOPMENT OF WIRELESS SENSOR NETWORK USING BLUETOOTH LOW ENERGY (BLE) FOR CONSTRUCTION NOISE MONITORING

Josie Hughes, Jize Yan* and Kenichi Soga
Cambridge University Engineering Department
Trumpington Street, Cambridge, CB2 1PZ, UK
*Email: yanjize@gmail.com

Submitted: May 5, 2015 ***Accepted: May 9, 2015*** ***Published: June 1, 2015***

Abstract- In this paper the development of a Wireless Sensor Network (WSN) for construction noise identification and sound locating is investigated using the novel application of Bluetooth Low Energy (BLE). Three WSNs using different system-on-chip (SoC) devices and networking protocols have been prototyped using a Raspberry Pi as the gateway in the network. The functionality of the system has been demonstrated with data logging experiments and comparisons has been made between the different WSN systems developed to identify the relative advantages of BLE. Experiments using the WSN for vehicle noise identification and sound location have further demonstrated the potential of the system. This paper demonstrates the versatility of a BLE WSNs and the low power consumption that is achievable with BLE devices for noise detection applications.

Index terms*:* Bluetooth Low Energy, Wireless Sensor Networks, Vehicle Noise Identification, Sound Localization, Construction Noise Monitoring.

I. INTRODUCTION

Wireless sensor networks (WSNs) are becoming a ubiquitous technology resulting from the development of low cost and low power wireless technology. WSNs are a group of spatially distributed sensing nodes with low maintenance requirements, which can automatically monitor environmental parameters and cooperatively transfer the data through a gateway to a main database using wireless networking [1]. There are a multitude of applications for WSN ranging from environmental monitoring to health care [2] [3].

Civil engineering is one area in which WSNs are having a significant impact with the development of 'smart infrastructure'. One application for WSNs is the monitoring of noise levels around construction sites to determine the noise pollution levels for surrounding residents, businesses and amenities. Such technology is currently required at London Bridge Station (Figure 1) which is undergoing significant renovation involving considerable construction activity [4]. This station has been identified as one of the busiest stations in the UK and provides an intersection between the rail and tube networks. The construction company requires a systematic solution to remotely monitor noise levels to determine if any changes in noise pollution are related to the construction activities.

Typically, noise levels below 80 dB are acceptable, but levels exceeding 90 dB become hard for people to tolerate for long periods of time. Sound measurements at the London Bridge Station redevelopment site indicated that construction noises from sources such as excavators and concrete mixers contributed to noise levels up to 86 dB [5]. However, the highest noise levels were found in areas subject to the noise from the railway, construction trucks and other vehicles, resulting in noise levels exceeding 100 dB (the red blocks in figure 1). As such, vehicle noise must be monitored closely as it contributes to the most harmful noise levels. Ideally, WSN technology would allow the identification and triangulation of vehicle noise, allowing the source of the noise to be determined.

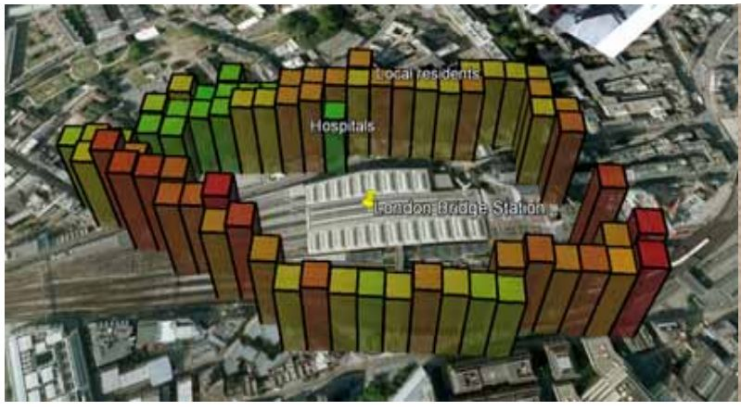

Figure 1. Sound map of measured sound levels around London Bridge Station showing highest sound levels occurred around high traffic areas [5].

This paper investigates the development of WSN systems for monitoring noise levels and environmental conditions for civil engineering applications, in particular investigating if WSNs can be used to identify and locate noise from vehicles. This requires a high sampling rate, whilst still maintaining low power consumption; a dynamic sensing challenge. The WSN developed uses Bluetooth Low Energy (BLE), the application of which is novel for noise monitoring applications.

Three prototypes nodes are presented and compared with consideration of power consumption, range and data rates, and their functionality demonstrated in data logging experiments. It is shown that a key advantage of BLE WSNs, is their low power consumption, which opens up the potential to integrate energy harvesting technology such as solar cells [6] and vibration energy harvesters [7] to extend the lifetime of the platform. Finally, early-stage vehicle identification experiments and sound location using triangulation demonstrations are presented.

II. BACKGROUND & THEORY

a. Wireless Sensor Networks

Wireless sensor networks (WSNs) comprise spatially distributed autonomous sensor ‘nodes’ which co-operatively pass their data through a network to the main ‘gateway’ in the system [8]. The networks have different topologies; common examples include star and mesh topologies [9]. Synchronization between nodes is important for dynamic sensing applications such as noise monitoring presented in this paper. Medium access control (MAC) protocols must be established to allow communication over the network by multiple devices and routing algorithms must be developed to create reliable and energy efficient package delivery [10].

WSN nodes have limited battery power, computation power and memory. As such, the key research challenges for wireless sensor networks are the efficient use of the limited resources whilst maximizing functionality and reliability. Other challenges include minimizing space considerations and achieving maximum range.

b. Vehicle Noise Detection using WSNs

Whilst there is considerable WSN research, there are currently only limited examples of WSN implementation for vehicle noise monitoring in civil engineering applications. There has been research into the development of WSNs for civil airport noise data collection [11] using a Zigbee wireless sensor network and an ARM noise data control module. The network uses a tree topology and utilizes multi-hop data transfer between nodes to enable data to reach the gateway. The system allowed the collection and transmission of airport noise data but the network suffered synchronization issues and struggled to achieve effective transmission of noise data.

The development of WSN for urban noise nuisance monitoring is another active research area. This research develops accurate sound maps using wireless networks together with acoustic sensors and off-the-shelf sensor nodes such as Tmote-Invent nodes and the Raspberry Pi to collect road traffic noise pollution data [12]. It was observed that the Raspberry Pi platforms are a feasible low-cost alternative to increase the spatial-temporal resolution, whereas Tmote-Invent nodes are not suitable due to their limited memory and low-performance audio recording. As such, ten Raspberry Pi platforms were distributed at different heights within a tower alongside a heavily used road. Zwicker's model of psychoacoustic metrics [13] was then applied to assess additional characteristics of noise traffic noise monitoring in comparison to simply considering the noise pressure level. In summary, further research and development into WSN for vehicle noise identification is required.

c. Networking protocols

Table 1 compares several key networking topologies used for short range wireless communication. Bluetooth and Zigbee protocols are used extensively for WSNs, however, both of these technologies have a comparatively high power consumption which severely limits the battery lifetime of nodes developed using these technologies. Additionally the data transmission rate of Zigbee is comparatively low, limiting the usage in dynamic sensing applications which usually require a high sampling rate and corresponding high data transmission rate. Bluetooth Smart, also known as Bluetooth Low Energy (BLE) or Bluetooth 4.0 is a newer protocol which has ultra-low power consumption and increased

communication range, and is aiming to replace Bluetooth Classic. Alongside the development of BLE, other low-power wireless solutions such as 6LoWPAN or Z-Wave [14] have been gaining momentum in applications, however these are mainly intended for applications that require multi-hop networking.

In this paper, BLE is the networking protocol investigated for noise monitoring applications as it provides the advantage of low power consumption whilst having reasonable data rates and range.

Table 1. Summary of Networking protocols [15][16][17].

	Max. Nodes per Master	**Peak Current Consumption**	**Range**	**Data Rate**	**Topology**	**Relative Cost**
Wi-Fi: IEEE 802.11b	32	~100mA	100m	54Mb/s	Star	Medium
Bluetooth	7	30 mA	10m	1Mb/s	Star	Low
ZigBee	100s	30mA	50m	250kb/s	Star, Mesh	Low
Bluetooth Low Energy	7+	15 mA	100m+	1 Mb/s	Star/Mesh Scatternet	Low

d. Bluetooth Low Energy (BLE)

BLE has ultra-low power consumption with a peak current consumption of only 15 mA and an achievable average power consumption of less than 1 uA for infrequent sampling [18]. The Generic Access Profile (GAP) controls connections and advertising of BLE and makes the device visible for connection [19]. BLE networks include the peripheral devices (the low power nodes) and a central device (the gateway) to which the peripheral devices connect. The peripheral device can set an advertising interval, and every time this interval passes, it will retransmit its main advertising packet. Alternatively, a listening device can request the response data. Peripheral devices must advertise themselves to allow a connection can be established.

The Generic Attribute Profile (GATT) defines the two way BLE data transfer and is used once a dedicated connection has been established using GAP. GATT transactions allow the transfer of data from a peripheral device to a central device, using a Bluetooth stack with three high-level objects: profiles, services and characteristics [20]. The profile defines the client/server relationship and services are used to break up data into logical entities which contain specific data called characteristics. Each service distinguishes itself from others using a unique numeric ID (UUID). The standard GATT maximum transfer unit is 23 bytes, three of which are taken up by the GATT protocol, leaving 20 bytes per transmission.

III. EXPERIMENTAL SECTION

Three WSNs have been prototyped (Table 1). Two of the WSNs developed use BLE, and for comparison the third uses WiFi.

Table 1. Summary of the node prototypes created, the network type, chip type and name.

Name	Network Type	Chip Type
Node A	Bluetooth Low Energy	RFD22301 (RFDigital)
Node B	Bluetooth Low Energy	BMD-200 (Rigado)
Node C	Wi-Fi	Spark Core

a. BLE Node Development (Node A & Node B)

An ultra-low power and high performance microcontroller is required for this application. There are number of System-on-Chip (SoC) manufacturers developing systems with a combined microcontroller and BLE transceiver. Comparing the main developers of BLE SoCs, Nordic Semiconductors are the leading producer of low powered, long life systems. Their BLE SoC, the nRF51822, utilizes an ultra-low power ARM Cortex-M0 and has an integrated 2.4GHz transceiver supporting Bluetooth Smart and Nordic Gazell 2.4 GHz, a proprietary network protocol that also allows inter-device communication enabling mesh networking [21]. The Gazell link layer is a robust wireless link that can be created between one 'host device' and eight connected 'devices'. A node can act as a host device allowing more sophisticated networks to be developed as a single device. These can communicate to multiple host devices and any node can change role and interface with a BLE communication [22]. This allows for the development of mesh networks.

The ARM Cortex-M0 is designed specifically for applications such as WSNs and has the smallest footprint of any ARM processor. The power consumption is ultra-low, and can be as little as 12.5μW/MHz [23]. The SoC has integrated sleep states that can be used to extend the battery life of a device and has limited on-board memory (128kB flash and 32kB RAM) and an on-board ADC.

Directly using the nRF51822 SoC package would require industrial equipment and techniques for integration into a PCB. To allow rapid prototyping, surface mount SoCs have been used which combine the nRF51822 and an antenna in a single package. Two different chips have been investigated.

The Node A prototypes have been produced using the RFD22301 produced by RFDigital (Figure 3a) which allows programming of the Cortex-M0 using the programming language C [24]. This SoC can be programmed and debugged using a five line connection to a USB

programmer. The pins have access to six additional general-purpose-input-output (GPIO) pins which can be configured as analog or digital input/output pins.

Node B is produced using the BMD-200 SoC developed by Rigado (Figure 3b) [25]. This can be programmed using the Keil MDK-ARM [26] and the Nordic Semiconductor Software Development Kit (SDK). A J-link Segger debug probe is used to download the firmware and allow debugging of the software [27]. This allows much greater control of the sleep states potentially achieving a much lower energy consumption. This also allows the development of a real time operating system that would also allow energy levels to be conserved.

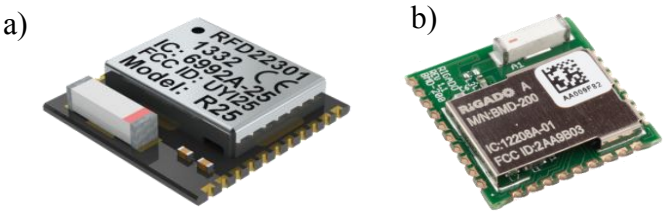

Figure 2. a) CAD model of the RFD22301 SoC used in Node A [24] b) Image of the Rigado BMD-200 SoC used in Node B [25]

All prototypes were developed using the same sensors. A microphone is used to provide a measurement of noise levels. Temperature and humidity sensors are also required for compensation, as noise levels vary significantly with temperature and humidity [28].

The ADMP401 MEMS microphone chosen is widely used in mobile phone device, and is a high quality, low power small sized MEMS device with an analogue output and omnidirectional sensitivity (Figure 2a) [29]. It has a high noise rejection ratio and high sensitivity, with a flat frequency response from 100 Hz to 15 kHz, and with a current consumption less than 250uA. A breakout board for the microphone has been used which also incorporates an operational amplifier providing a gain of 67.

The LMT86LP analogue temperature sensor has been used. This device has a wide sensing range of −50°C to 150°C and an accuracy of ±0.25°C [22]. The sensor has a low quiescent current of 5.4 μA resulting in low power consumption and is available in a 3-lead through hole package (Figure 2b). Although amplification could be used to increase the resolution of the sensor this would increase the complexity, size and efficiency of the circuitry and as such is unnecessary for this application.

An analogue humidity sensor has been chosen over a digital sensor as they provide a higher accuracy at a lower cost. The analogue sensor chosen is a Honeywell HIH-5030-001 (Figure 2c) and has the accuracy of ±3% [30]. The sensor was specifically

chosen as it operates at low voltages, down to 2.7 V, which is lower than many other widely used humidity sensors. A typical current draw of the device is 200 μA. The sensor is provided in a three-leg surface mount package.

Figure 3. a) MEMS Microphone and associated breakout board [29] b) LMT86LP Temperature Sensor [31] c) Surface mount, 3 pin Honeywell Humidity Sensor [30].

b. BLE Network Structure (Node A & Node B)

For the two BLE prototypes (Node A and Node B) the same BLE network has been employed. For the gateway, a Raspberry Pi single board computer has been used. This is a low cost, low power Linux-based system that, in this case, is running the operating system Raspian. BlueZ, a Linux Bluetooth protocol stack, is used on the gateway to provide support for the Bluetooth layers and protocols. This allows connections to be made to BLE devices and GATT requests sent. A BLE enabled USB 'dongle' is connected to the Raspberry Pi, allowing communication with BLE devices. The BLE USB dongle port must first be opened and initialized after which the low energy connections can be made. The schematic of the network architecture is given in Figure 4.

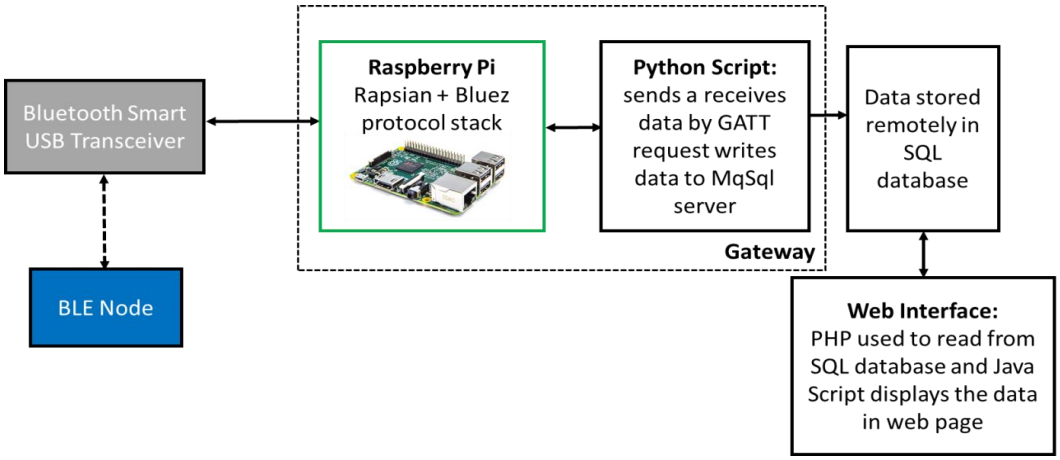

Figure 4. BLE Network architecture used with Node A and Node B showing the node, Raspberry Pi Gateway and post processing.

A Python script has been developed to send and receive data to the Raspberry Pi using non-interactive GATT requests. A class has been made which allows data to be sent and received from the Pi. Different instances of the class can be created; allowing data to be transferred from different MAC addressed devices. The data is transmitted in hexadecimal as a single 20 byte string, converted into decimal and then split into the relevant sensor information. To store the data, it is then written to a text file and to a SQL database. PHP is then used to read the data from the SQL database after which JavaScript and Highcharts libraries [32] are used to create interactive graphs for real time display of the data.

c. Node A (RFD22301) Prototype Development

During the development of Node A using the RFD22301, the SoC was initially tested by creating a breakout board to ensure that it is possible to establish communication. Proteous PCB software has been used to design the circuit and PCB layouts.

The sensors are connected to the GPIO ports on the SoC, and a five pin header has been connected to the relevant pins for programming and debugging. As for all the nodes, four AA batteries are used as a power source. A 3.3 V regulator is used to provide a consistent voltage which is within the range required by the SoC and the sensors, allowing a single power rail to be used. Additional capacitors have been added to reduce the voltage ripple and ensure the stability of the output.

A DS1307 Real Time Clock (RTC) [33] has been added to allow synchronization of the devices and time stamping of the data. This is a serial, low power clock and calendar chip counting seconds, minutes and hours. It uses an I2C serial interface, so is connected to two GPIO pins on the SoC via pull-up resistors. A standard 32 kHz quartz crystal is required and a voltage must be applied to the external power pin to simulate the presence of a back-up battery supply. The final PCB is given in Figure 5.

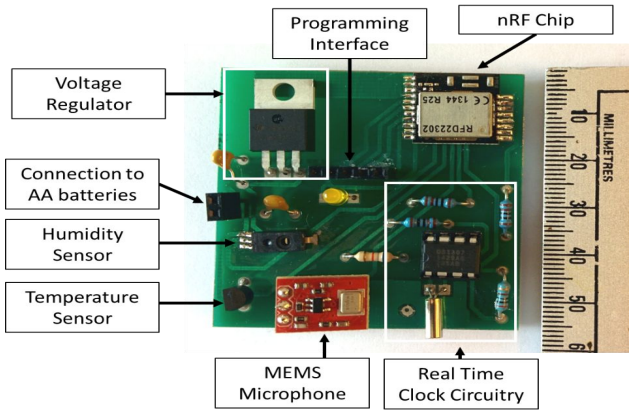

Figure 5. Node A PCB with components assembled with key parts labelled.

1) Sensor Calibration

After producing the sensor nodes, the sensors were calibrated. The temperature sensors were calibrated against a commercial temperature probe with the accuracy of ±0.1°C. The device and the temperature probe were both waterproofed and then placed, together, in hot water. Data was then taken from the probe and the wireless device as the water cooled, with the device temperature determined by averaging over twenty readings to minimize noise. The results are given in Figure 6, and show that the relationship between sensor reading and temperature was highly linear. The conversion between temperature and sensor reading was determined as a linear function.

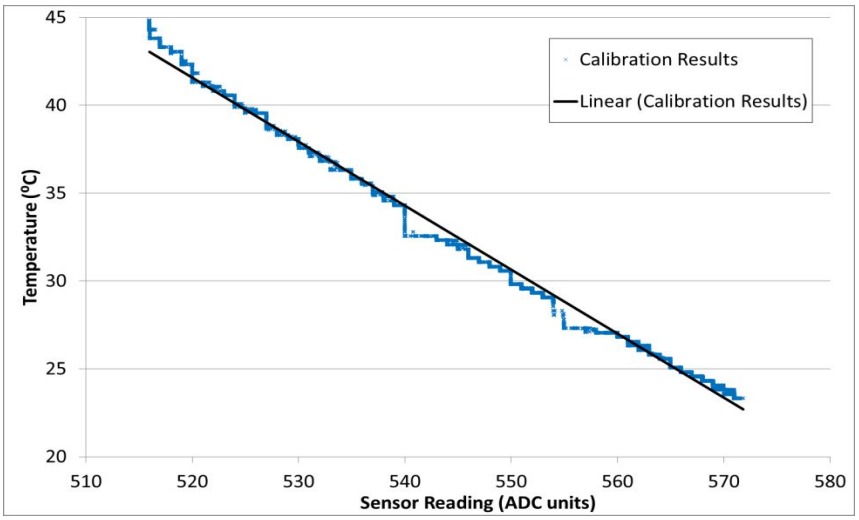

Figure 6. Results from temperature calibration experiment showing the variation in temperature sensor readings from the node with measured temperature.

Similarly, the humidity sensor was calibrated by placing the device and a commercial humidity sensor (accurate to ±1%) in a closed container. Steam was introduced into the closed contained and the humidity levels from both measured. The results are given in Figure 7. A quadratic relationship was used to map sensor reading to percentage humidity.

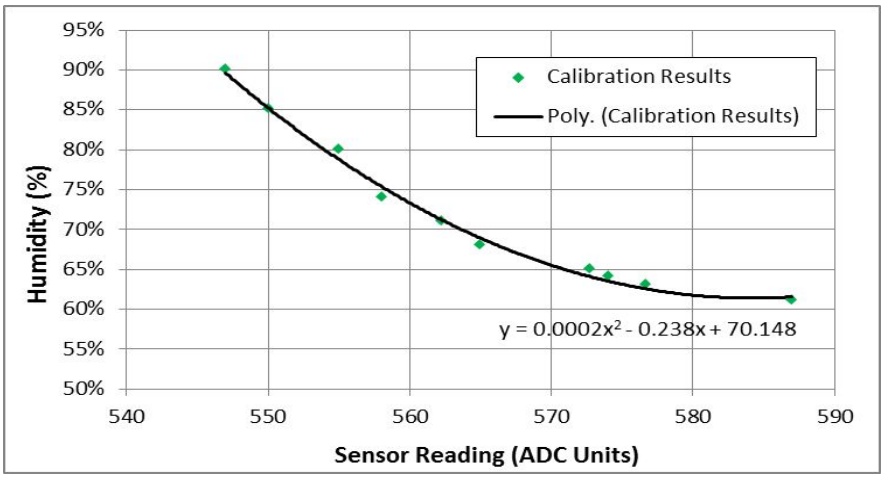

Figure 7. Results from humidity sensor calibration experiment with measured humidity plotted against humidity measured from the on-node humidity sensor with a polynomial trend line shown.

The measured analog signal from the MEMS microphone was converted into Sound Pressure Levels (SPL) using:

$$SPL = 20log_{10}\left(\frac{Output \times P_{ref}}{Amplification \times Sensitivity}\right)$$

Output – microphone reading in millivolts

Pref – reference sound pressure in air (commonly 20 μPa)

Amplification – amplification of any circuitry used (*A*=67)

Sensitivity – sensitivity of the microphone in millivolts per Pascal

Calibration was performed using a single Node, and was assumed to be the same for all devices produced.

2) Wireless communication

To test the wireless communication of the BLE Node A devices, three of the nodes were placed in different environmental conditions and the sensor readings logged. The first device was placed outside, the second on a radiator within in one room, and the third in a center of an adjoining room. The temperature, humidity and sound levels have been captured over a period of time.

Figure 8 shows the results from a temperature logging experiment. The radiator was switched on at 8:20 resulting in an increase in the radiator temperature node until the radiator was switched off at 9:25 after which the temperature slowly lowers. Comparing this to Device 3, it can be seen that there is a gradual increase in room temperature when the radiators are

switched on which levels off after the radiators are switched off. The outside temperature is considerably lower than the indoor temperature as expected and remains reasonably constant.

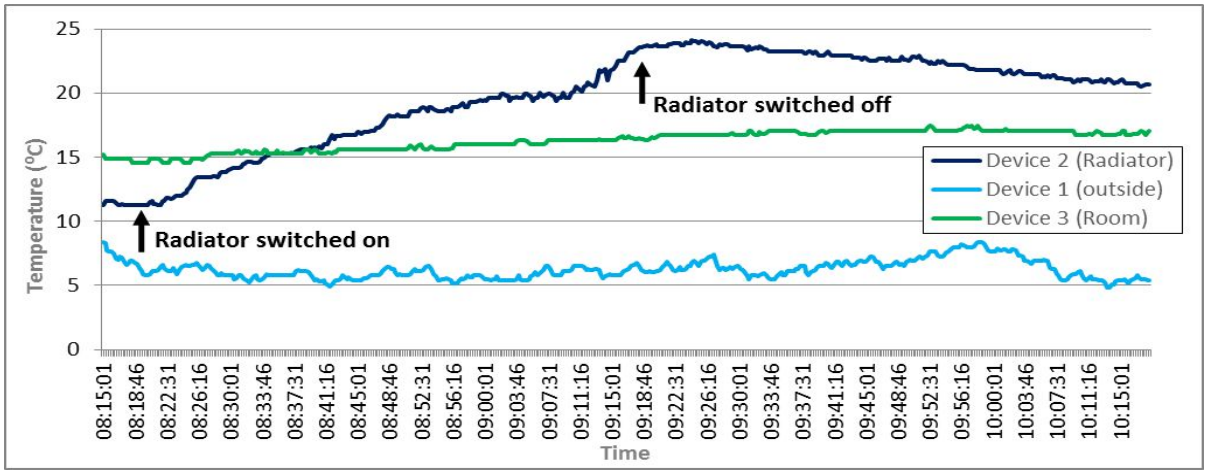

Figure 8. Temperature sensor data from three nodes placed in different locations plotted over time.

The same calibration results were used for all the nodes, however, as shown at the start of the experiment there is discrepancy between measured temperature at points at which they should have the same temperature. To achieve a more representative result the nodes should be calibrated individually.

Figure 9 shows the results from the humidity sensors. The results show a slight initial increase in inside humidity after which it then drops. Outside, the humidity is consistently higher as expected due to the wet conditions outside.

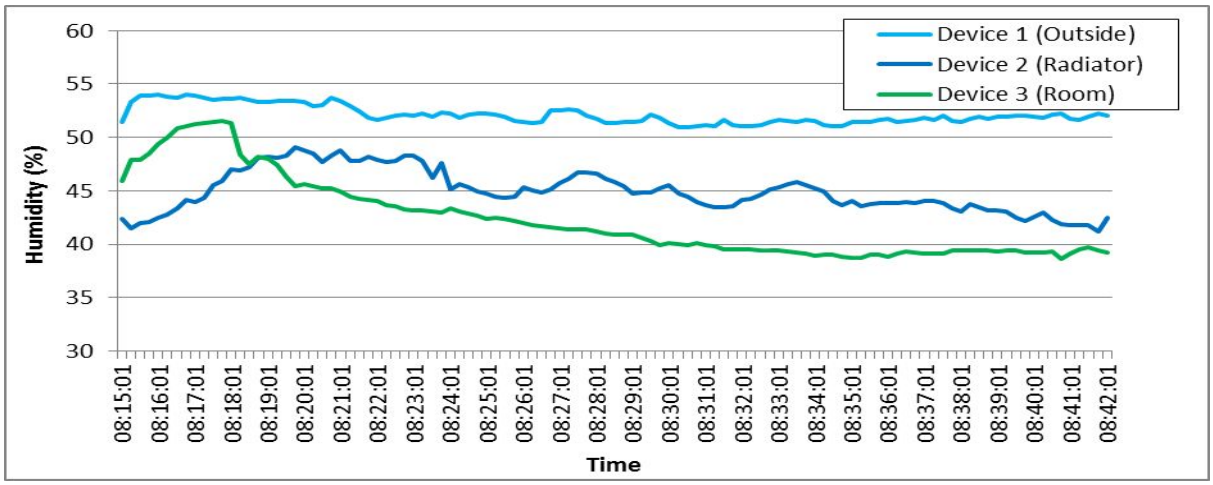

Figure 9. Humidity sensor data from three nodes in different locations plotted over time.

The varying sound levels are given in Figure 10. The two indoor sensors show similar correlations, with similar increases in sound levels, in particularly at sound events around 8:33. There is an increase in sound levels of all three sensors at 8:49 due to movement of people from outside to inside the building.

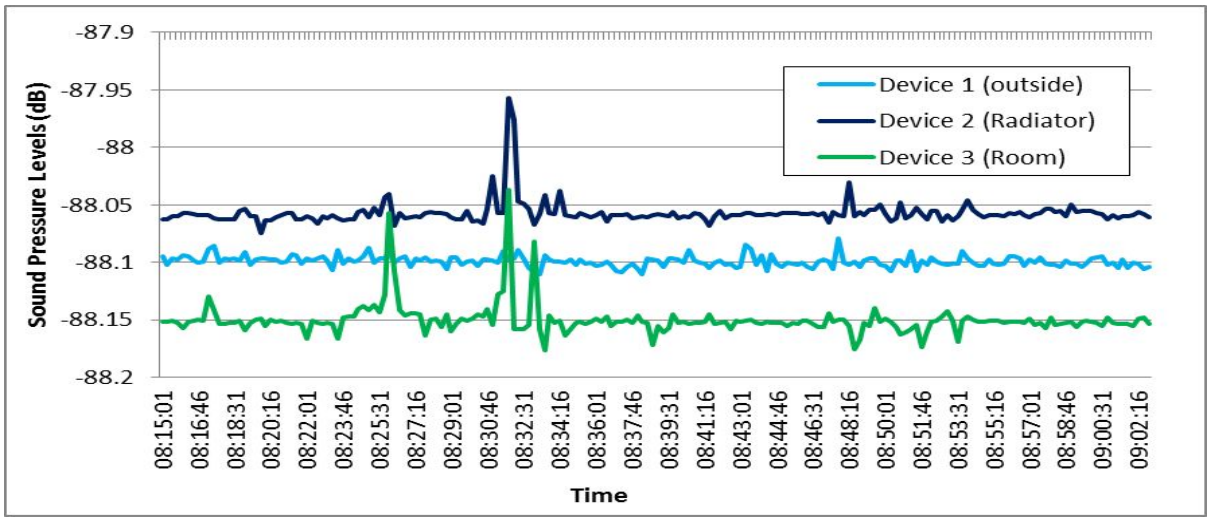

Figure 10. Sound data from three nodes in different locations plotted over time.

These results demonstrate that the prototype can be used for data logging and that the system developed allows continuous monitoring of sound and environmental conditions over time, in a range of conditions and over a spatial area.

3) Software Development

The software has been designed to be power efficient. To start data transmission the gateway sends a timing signal to all of sensor nodes. The time stamp is used to update the real time clocks on all of the nodes using I2C to synchronize the devices. Asynchronous requests from the Raspberry Pi are then send out to the sensor nodes by sending GATT requested to the MAC addresses of the different sensor Nodes. A moving average of the sensor readings is calculated and these are transmitted on receipt of the request. The nodes are resynchronized periodically, with time stamps sent from the Raspberry Pi. A summary is given in Figure 11.

To minimize power consumption, the nodes are kept in sleep mode while waiting for the request from the Raspberry Pi. On receiving a message over BLE, an internal pin is used to wake the system from sleep mode such that it can transmit the data. All of the exposed pins are being used; hence an internal pin must be used. Low-level commands were used to toggle an internal pin pull-up to simulate a pin high connection triggering the wake from sleep mode, after which the pin can then be toggled down.

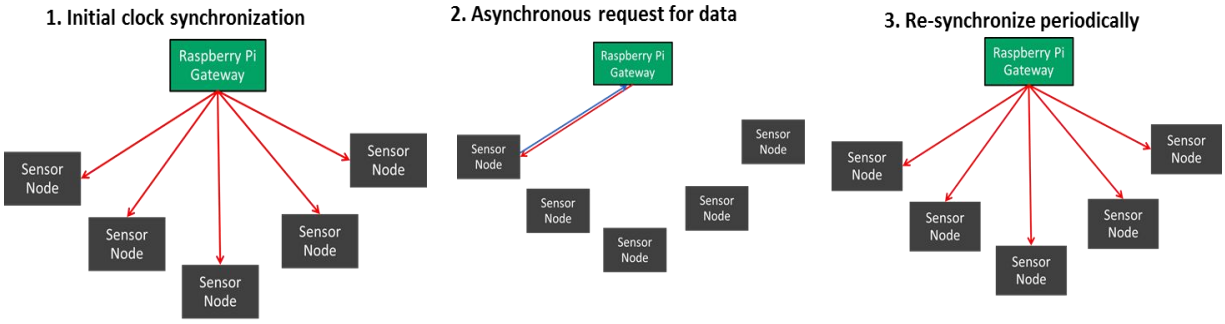

Figure 11. Summary of synchronization used in the software to synchronize the motes; initial synchronization, asynchronous requests from data and period re-synchronization.

4) Node Case Design

To house the node and power supply a case was designed. The case needs a good air flow through it to allow the sensors to accurately read the current conditions. The box was developed using the CAD package Creo and printed using a MakerBot 3X in ABS plastic (Figure 12).

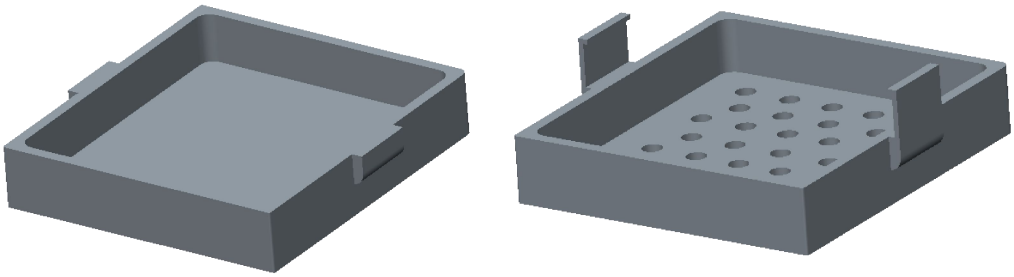

Figure 12. CAD modes of the housing designed for the sensor nodes.

The final PCB with all components assembled is shown with the batteries with the designed box in Figure 13. The holes align with the area in which the sensors are mounted below to allow air flow to the sensors to obtain representative readings.

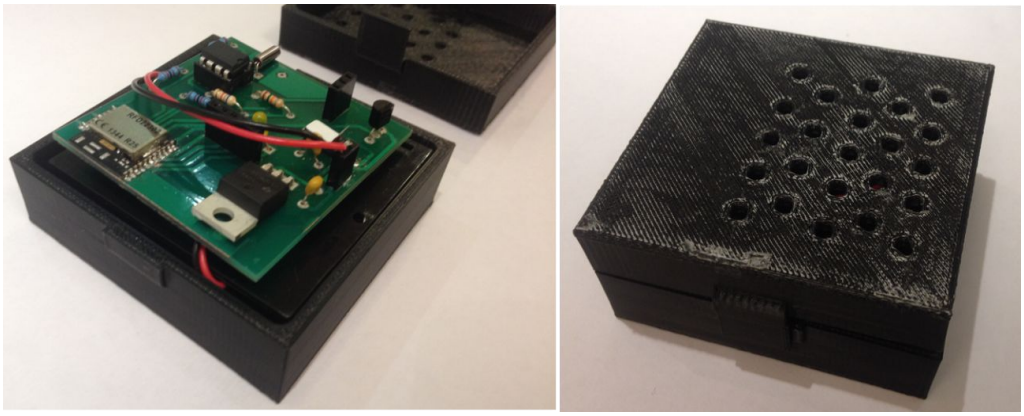

Figure 13. Image of the finished node and batteries in the 3D printed case.

d. Node B (BMD-200) Prototype Development

A node has also been developed using the Rigado SoC. A break out board was first produced with the SoC and headers attached to allow testing and establish communication with the chip. Using the nRF development software the chip could be initialized and then firmware developed and loaded using the ARM Keil µvision software and Nordic Semiconductor libraries. Libraries for analog read and I2C communication were developed.

The software developed allows much lower control of the sleep states such that the node can be put into deep sleep when not transmitting, significantly reducing power consumption.

After testing, a PCB has been designed for this chip, with the sensors attached to the designed input ports. This system can be used in the same network developed for the previous SoC, with the correct MAC address and UUID's set.

e. Node C (Wireless Node) Development

For comparison, a wireless node has been developed using a Spark Core. This is an open source development board that uses a Texas Instruments CC3000 Wi-Fi module using the IEEE 802.11 WiFi Standard and an ARM Cortex-M3 micro-controller [26].

A PCB has been developed which has on-board power regulation regulating the 8V supply down to 5V. In addition, the sensors are connected to GIPO ports configured as analogue inputs, and headers added for connections to the Spark Core (Figure 14).

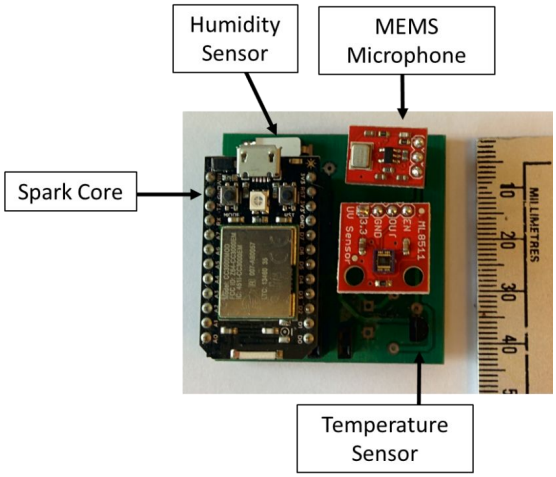

Figure 14. PCB produced for Node C (WiFi Node) fully assembled.

A similar network architecture to that used for the BLE devices was developed. The WiFi board can be configured to connect to a wireless network using a Wi-Fi Protected Access 2-Pre-shared Key (WPA2 PSK) encryption over IEEE 802.11. It is then possible for the sensor readings to be uploaded from the node to the cloud. Using a Python script API requests can

be used to obtain the data after which they can be stored in a database and displayed using PHP and JavaScript as shown in Figure 15.

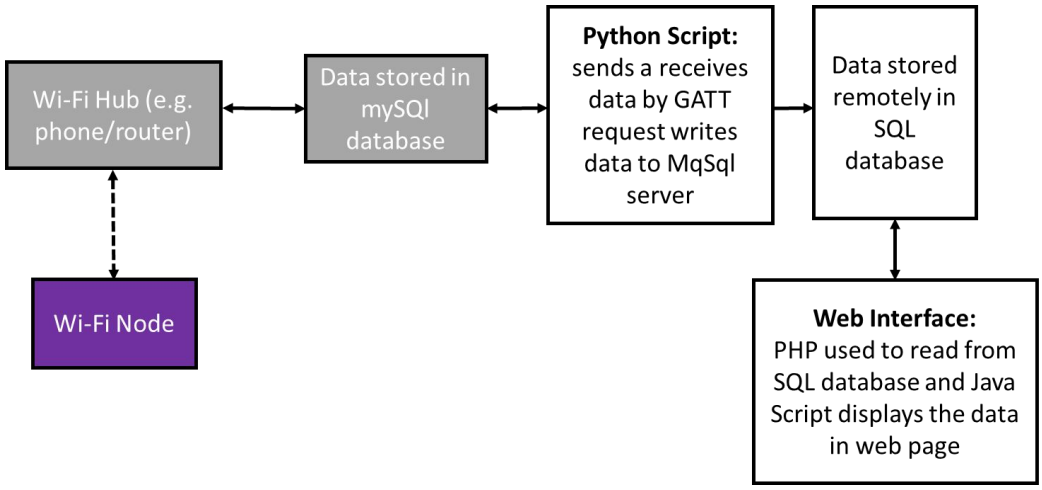

Figure 15. Overview of network architecture used for Node C (WiFi Node) showing the node, Raspberry Pi gateway and post processing.

IV. RESULTS & DISCUSSION

The results are presented in two parts. Firstly, the performance of the devices developed are presented and compared. Demonstrations of sound locating and vehicle identification using Node A are then discussed.

a. Performance Metrics

1) Power

To investigate the power consumption of the devices, a power monitor was used which allows real time capture of the voltage and current, and hence power consumption, of the device [27]. The waveforms can be observed, and the average characteristics determined. The average power consumption and current for a given voltage has been measured with a fixed 20 byte packet transmission every second. The lowest operation voltage of the device is measured to be 2.4 V using the power monitor. The power consumption of the three WSN nodes is given in Tables 3, 4 and 5.

Table 3. Power consumption for Node A (RFD22301).

Voltage (V)	Power (mW)	Current (mA)
3.2	21.92	6.85
3.0	19.05	6.35
2.8	16.55	5.91
2.6	14.17	5.45
2.4	11.19	4.96

Table 4. Power consumption for Node B (BM-200 Rigado SoC)

Voltage (V)	Power (mW)	Current (mA)
3.2	3.15	0.99
3.0	3.09	0.97
2.8	2.69	0.96

Table 5. Power consumption for Node C (WiFi Mote).

Voltage(V)	Power(mW)	Current(mA)
2.55	277.14	60.98

Using the minimum power consumption that has been measured for each of the nodes the lifetime of the nodes can be estimated for the four AA battery power supply used, assuming each AA battery is rated at 2500 mAh.

Table 6. Estimated lifetime of nodes with 4 AA batteries.

Platform	Estimated Lifetime
Node C: WiFi Mote	7 days
Node A: RFD22301	84 days
Node B: Rigado SoC	434 days

The BLE devices have considerably lower power consumption than the WiFi device, resulting in a significantly longer lifetime. As expected, Node B shows the lowest power consumption, which is of the order of milliwatts. The consumption during sleep mode was measured at 0.4 mW, therefore if the transmission window were to be reduced, for example transmitting every 10 seconds, then the power consumption could be reduced significantly to achieve this goal.
Node B shows reasonable power consumption and it is much improved on results reported for Classic Bluetooth or ZigBee, however the limited control of sleep states has led to a higher power consumption. Further software development could allow power consumption to be reduced.

2) Range

The range of the BLE Node A was tested by increasing the distance between the node and the gateway until communication was no longer possible. A comparison is then made to the WiFi node. The range has been determined for different transmitting powers ranging from -20 dBm to +4 dB with the results given in Figure 16. The range can also be plotted against the

power consumption of the device; this is shown in Figure 17. These results were obtained inside a room, in free space. In outside areas with no walls and hence fewer reflections, these ranges should be greater.

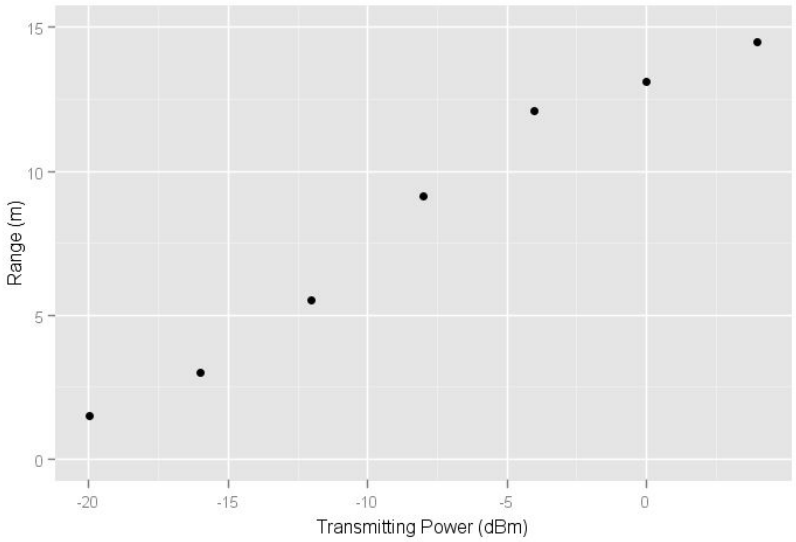

Figure 16. Variation in range of the node to gateway communication as the transmission power of the BLE transceiver is varied.

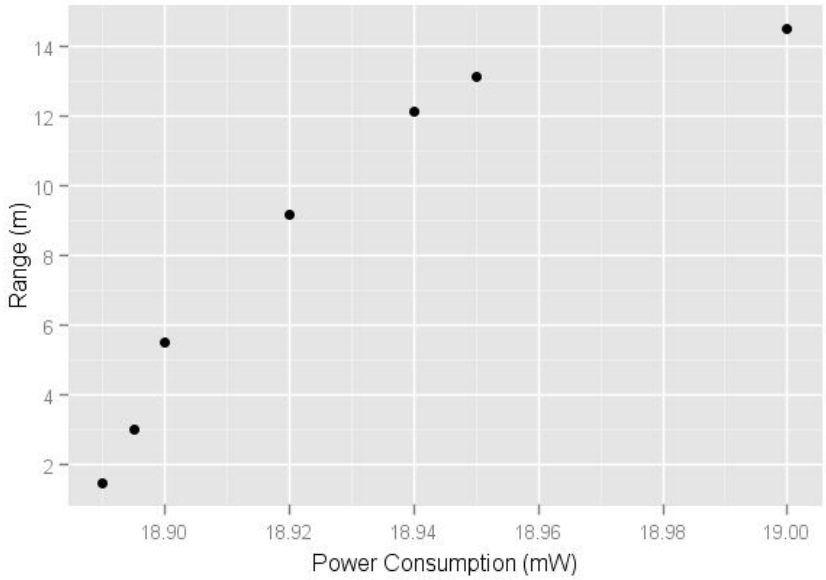

Figure 17. Variation in node to gateway range as the power consumption of the node is varies.

The results show that an increase in transmission power leads to an increased range; however, as expected the rate of increase reduces as the power is increased. Equally, for power consumption the relationship between range and power consumption is not linear. As the range increases, greater power consumption is required to extend the range.

This range is reasonable for short range applications however, Bluetooth Smart has a maximum possible range of 100 feet in ideal conditions [11]. Using an alternative antenna, other than provided which the chip, could help extend the range of the device, using PCB antennas of larger size could improve the range achievable. Additionally changes could be made to the layout of the PCB, to increase the distance from the copper plating and the antenna, however, this would require the size of the node to increase. In comparison the WiFi node had a maximum range of 30 m, but uses more power. Despite having twice the range of the BLE node requires over 10 times the power. The range could be potentially extended by using a point-to-point network with repeaters.

3) Data transmission rate

The data transmission rate was tested by determining the time taken for 1000 connection events each of the maximum packet size (20 bytes). For BLE, the fastest theoretical data transmission rate is 1 Mbps. The experimental results are given in Table 7.

Table 7. Data transmission rate of the different nodes.

Node	Maximum Data Rates (kbps)
Node A (RFD)	10.5
Node B (BN-300 Rigado)	12.0
Node C (WiFi)	1200.0

The measured data rate results are considerably lower than the theoretical maximum. Potential reasons for this include a limit in the number of application layer messages a device can send per connection event (due to memory limitations) and processing delays. The Spark Core had a considerably higher data rate, over a factor of 100 greater than that of the BLE devices. As shown previously, this is at the expense of the considerably higher power consumption.

The data rate is also dependent on the receiving device, and the connection interval that is set on the BLE dongle. If the connection interval could be reduced to the lowest possible value, 7.5 ms, this would allow data rate to increase. The results show that BLEs strength, and indeed what it was designed for, is the efficient transmission of small messages infrequently opposed to high data transmission rate.

b. Functionality Testing

1) Received Signal Strength Indicator (RSSI)

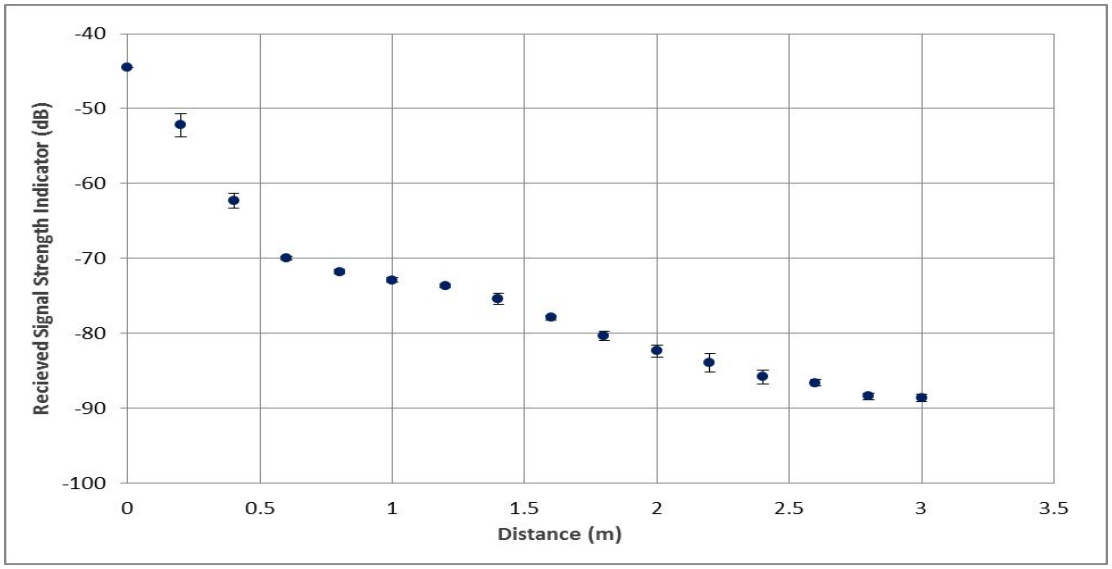

Figure 18. RSSI Experimental results, showing the RSSI value returned by the node at varying distances when -8 dB transmission power is used.

Received signal strength indication (RSSI) is a measure of the power of the received radio signal, and can be used to estimate the distance between the node and the gateway. On receiving a message from the gateway the node can determined an RSSI value in decibels. A conversion between this RSSI value and distance can be made to estimate the distance of the node from the gateway.

Figure 18 shows the RSSI values measured with varying distance from the gateway for -8 dBm power transmission. These show that it is possible to determine the distance the nodes are from the gateway using the RSSI, however, the precision that can be determined reduces with distance from the gateway.

The variation in RSSI values was also tested with high transmitting powers; however, it was found that with higher transmission power, the signal was more susceptible to interference from other similar frequency transmissions fading effects and reflections. A power of -8 dBm provided the best compromise of range and minimal interference.

If two or more nodes are used triangulation can be used to determine the relative positioning between the nodes and the gateway, making use of the Gazell networking capabilities of Nordic SoC devices. Detecting changes in RSSI could also be used detect if a node has been moved.

2) Sound localization

One application for which the WSNs could be used is to triangulate, or locate, sounds using multiple nodes. Locating a sound can assist with attributing it to a particular source and hence is useful for noise identification on construction sites. This requires high frequency sampling and accurate time stamping of the data.

The nodes were separated by 6 meters, and a sound source placed at given distances between the nodes. By accurately time-synchronizing the nodes, the time difference between of the nodes detecting the peak sound signal can be used to determine the location of the between the nodes. This does require significant post-processing of results, and long term, this would be best performed on the network gateway or once the data is stored in the SQL database.

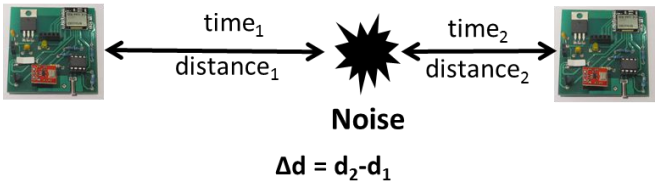

Figure 19. Experimental design for initial experiment using the nodes to determine the location of sounds in 1D.

Using the time difference, Δt, the difference is distance can be calculated using:

$$\Delta distance = speed\ of\ sound \times \Delta t$$

The experiment was repeated five times, and the results of measured difference against the true distance are given in Figure 20. The average results are plotted with error bars representing the standard deviation. The results show a linear variation in distance with measured distance. There is a zero offset, but the relationship is linear. However, the standard deviation demonstrated by the error bars is significant, showing a considerable variation in results.

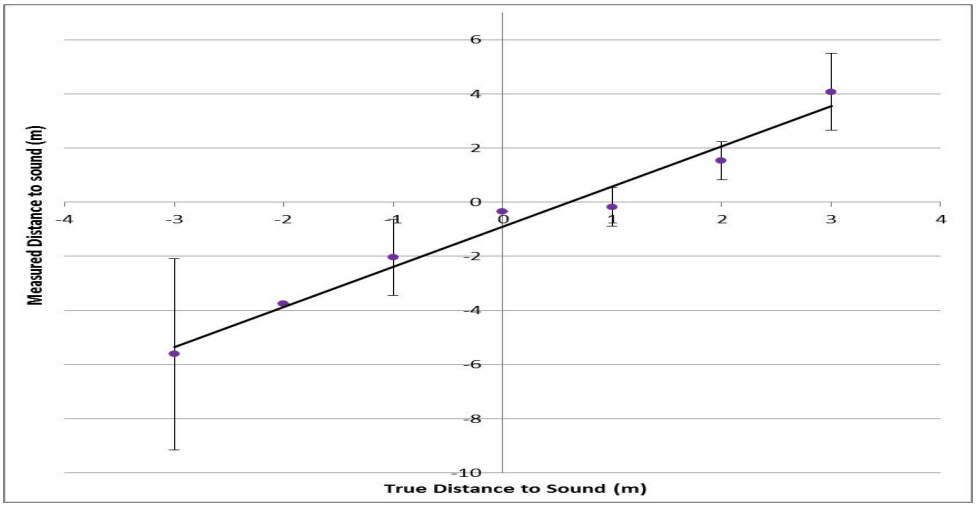

Figure 20. Measured distance, as determined by the nodes plotted against true distance.

The sampling rate used is limited at 500 Hz, which gives a resolution of 0.8 meters. As such the results obtained give a good indication of the location of the sound, with the errors bars showing a variation which would be expected given this resolution.

This has demonstrated that, in principle, the devices can be used to estimate the location of a sound. If the distance between the nodes and the sampling frequency could be increased, the accuracy of the located sound source could be increased.

3) Vehicle noise identification

A node was positioned 1 metre from a road, and was used to wirelessly record the sound levels. The maximum possible sampling rate was used (approximately 500 Hz), which is limited by the maximum sampling rate of the analogue to digital converter (ADC) as well as the maximum data transmission rate that could be achieved. The sound profiles detected by the nodes are given in Figure 21 and show that vehicles are easily identifiable as sound 'events'. For single vehicle events such as this, even simple 'thresholding' could be sufficient to identify a vehicle and potentially the type of a vehicle. Although this could be used in situations where there are few of vehicles, and low background noise, more complicated setting could require more advanced algorithms and a larger number of nodes. Methods such as machine learning could be used to develop algorithms that would allow the detection of specific vehicle types and identify between different types of noise such as that from construction and that from non-construction sources.

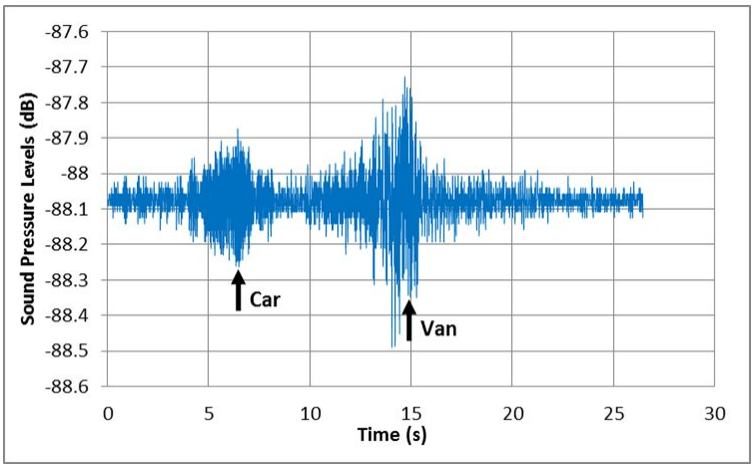

Figure 21. Measured sound levels for different vehicle types using the node microphone.

V. CONCLUSIONS AND FUTURE DEVELOPMENT

The prototypes developed have demonstrated that BLE is a viable and useful technology for WSN applications in construction noise monitoring. A key advantage of the system developed is the potential for low power consumption, with a power consumption of 2.69 mW at 2.8 V was achieved using Node B. Further software development and increasing the data transmission window could allow the power consumption to drop to 1 mW, this would allow energy harvesting techniques to be used to extend the battery life of the device. The maximum range of the BLE nodes have been found to be 15 metres, almost half that of the range of the WiFi node. Given the potential size of construction sites, this range is low. As such, many repeater nodes may be required to extend the range of network over a whole site. With improvements in the PCB layout or using a by higher range antenna, a range of 30 meters should be achievable in free-space.

The WSN allows the wireless data logging of the environmental and sound conditions. The entire system, from sensors to data storage and display has been designed and tested demonstrating a 'proof of concept'. Although the WSN has been used for the specific application of construction site noise monitoring, there is considerable scope for further applications of the system that make use of the key advantages of the system developed.

The potential to use the system for determining the location of sounds has been shown to work in one dimension. The accuracy and precision could be improved by using higher sampling rates and increasing the distance between the devices. Using more nodes would also allow for the triangulation of sounds, which could be used to assist with locating the sources of noises on construction sites. Additionally, the ability to detect vehicles using the system has been demonstrated. The strength of BLE is the ease of connectivity and the ultra-low sleep power consumption and this can only be capitalized on if the transmission window is large.

This project has demonstrated the feasibility of the component parts of a WSN for construction noise monitoring in applications such as the London Bridge Station Redevelopment project. The techniques and system presented could be used to assist with the identification and location of the source of vehicle noise on construction sites. With further developments and improvements the system could be used with energy harvesting technology to provide a self-sustaining noise pollution WSN, this is a key advantages of the system as would allow it to be used for long periods with minimum human-intervention.

a. Future Development

For node A, developed with the RFD22301 SoC, further software improvements to minimize power consumption should be investigated. One method to decrease power consumption would be to use the real-time-clock (RTC), which can be set to trigger a pin high, to wake the device from sleep. Node B, developed with the BN-300 SoC, had a lower power consumption and 1mW power consumption could most likely be achieved by reducing the data transmission rate. Again, using a RTC to wake the chip may also help reduce power consumption. Also, using a real-time-operating system (RTOS) may allow greater control of the power consumption when sleeping so could be used to help minimize energy consumption. The size of the nodes could be reduced significantly by using surface mount components with smaller footprints. This would make the devices easier to position within a construction environment. Additionally, the range of the nodes could be increased by using an alternative external antenna; this could enable the range to be doubled. This could also be increased by using intermediary relay nodes, such that a string of devices can be used over a larger area. Increasing the range even minimally would help as construction sites are often large and good coverage is required.

For the localization of sounds and the detection of different vehicle types, high frequency sampling is required. Currently this is limited by both the sampling rate of the ADC and the maximum data transmission rate. Vehicle noise is in the range of 1-4kHz. Nyquist's theorem states that the sampling rate should be at least twice the maximum frequency response; therefore ideally a sampling rate of at least 8kHz should be used, which is unachievable with the current system. However, methods such as compressive sensing could be used to allow reconstruction of the signal whilst sampling at a lower frequency [34].

The use of digital sensors could allow faster acquisition of data from the sensors. Also, a microcontroller with integrated digital signal processing (DSP) unit could be used. This would allow much of the noise analysis to be performed on the node, potentially reducing the data transmission frequency that would be required. This would be at the expense of high chip power consumption; however, this is minimal in comparison to the power consumption of data transmission.

Initial tests have demonstrated that the system can be used for data logging applications, however, further work testing the system in outdoor conditions on construction sites and for long periods of time is required to ensure the reliability and robustness of the system.

VI. ACKNOWLEDGMENTS

This project was funded by the EPSRC CDT in Sensor Technologies and Applications (Grant EP/L015889/1). In-kind support was also obtained from Costain London Bridge Station Redevelopment project. Special thanks go to Prof Jian Kang and Dr Ming Yang at the University of Sheffield for the valuable discussion of the noise detection.

VII. OPEN DATA STATEMENT

All data accompanying this publication are directly available within the publication.

REFERENCES

[1] F. Akyildiz and I. Kasimoglu, "Wirless Sensor and Actor Networks: Research Challenges," *Ad Hoc Networks,* vol. 2, no. 4, pp. 351-367, 2004.

[2] D. Puccinelli and M. Haengii, "Wireless Sensor Networks: Applications and Challenges of Ubiquitous Sensing," *IEEE Circuits and Systems Magazine,* vol.5, no. 3, pp. 19 - 31, 2005.

[3] M. Othman and K. Shazali, "Wireless Sensor Network Applications: A Study in Environment Monitoring System," *Procedia Engineering,* vol. 41, pp. 1204-1210, 2012.

[4] Network Rail, "London Bridge Redevelopment," [Online]. Available: http://www.networkrail.co.uk/aspx/12179.aspx. [Accessed 3 May 2015].

[5] Z. Xiao, "Centre of Smart Infrastructure and Construction (CSIC) Demonstration Report: London Bridge Station", *UROP report*, University of Cambridge, 2013.

[6] H. Kim, Y. Min, C. Jeong and K. Kim, "A 1-mW Solar-Energy-Harvesting Circuit Using an Adaptive MPPT With a SAR and a Counter," *Circuits and Systems II: Express Briefs,* vol. 60, pp. 6331-6335, 2013.

[7] Y, Jia, J. Yan, K. Soga and A.A. Seshia "A parametrically excited vibration energy harvester," *Journal of Intelligent Material Systems and Structures,* vol. 25. pp. 278-289, 2014.

[8] F. Akyildix and I. H. Kasimoglu, "Wireless Sensors and Actor Networks: Research Challenges," *Ad Hoc Networks,* vol. 2, no. 4, pp. 351-365, Oct. 2004.

[9] C. Buratti, A. Conti, D. Dardari and R. Verdone, "An Overview on Wireless Sensor Networks Technology and Evolution," *Sensors,* vol. 9, no. 9, pp. 869-6896, 2009.

[10] C. E. F. A. I Demirkol, "MAC Protocols for Wireless Sensor Networks: A Survey," *IEEE Communications Magazine,* pp. 115-121, April 2006.

[11] X. Zang and W. Ren, "Wireless Sensor Network Based on Airport Noise Data Collection System," *The Open Electrical & Electronic Engineering Journal,* vol. 8, pp. 90-93, 2014.

[12] J. Segura-Garcia, S. Felici-Castell and J. Perez-Solano, "Low-Cost Alternatives for Urban Noise Nuisance Monitoring Using Wireless Sensor Networks," *IEEE Sensors Journal,* vol. 15, no. 2, pp. 836 - 844, 2015.

[13] H. Fastl and E. Zwicker, Psycho Acoustics: Facts and Models, Berlin: Springer, 1990.

[14] J. Hui, D. Culler and S. Chakrabarti, "6LoWPAN: Incorporating IEEE 802.15.4 into the IP architecture," *Internet Protocol for Smart Objects (IPSO) Alliance*, 2010.

[15] Habib F. Rashvand, Ali Abedi, Jose M. Alcaraz-Calero, Paul D. Mitchell, and Subhas Chandra Mukhopadhyay, Wireless Sensor Systems for Space and Extreme Environments: A Review, *IEEE Sensors Journal,* vol. 14, no. 11, pp. 3955-3970, 2014

[16] Ls Research, "Integrated Transceiver Modules for ZigBee / 802.15.4 (2.4 GHz)," *ModFlex*, 2012.

[17] Bluetooth, "Bluetooth Smart Technology: Powering the Internet of Things," December 2014. [Online]. Available: http://www.bluetooth.com/Pages/Bluetooth-Smart.aspx. [Accessed 20 March 2015].

[18] R. Nilsson, "Low energy Bluetooth wireless protocol," *Control Engineering,* 2012.

[19] Bluetooth Special Interest Group, "Bluetooth Developer portal," 2015. [Online]. Available: https://developer.bluetooth.org/TechnologyOverview/Pages/Profiles.aspx. [Accessed March 2015].

[20] C. Gomez, J. Oller and J. Paradells, "Overview and Evaluation of Bluetooth Low Energy: An Emerging Low-Power Wireless Technology," *Sesnors (Basel),* vol. 12, no. 9, pp. 11734-11753, 2012.

[21] Nordic Semiconductor, "nRF51822: Multiprotocol Bluetooth low energy/2.4GHz RF System on Chip," *Nordic Semiconductor ASA*, 2014.

[22] Nordic Semiconductor, "nRF51 SDK: Gazell Link Layer User Guide," 6 March 2015. [Online]. Available: https://developer.nordicsemi.com/nRF51_SDK/nRF51_SDK_v8.x.x/doc/8.0.0/s110/html/a00112.html. [Accessed 5 May 2015].

[23] ARM, "Cortex-M0 Processor," 2014. [Online]. Available: http://www.arm.com/products/processors/cortex-m/cortex-m0.php. [Accessed 5 May 2015].

[24] RF Digital Corp, "http://www.rfdigital.com/index.html," 2014. [Online]. Available: http://www.rfdigital.com/index.html. [Accessed 30 April 2015].

[25] Rigado, "Rigado: BMD-200," 2014. [Online]. Available: https://www.rigado.com/product/bmd-200/. [Accessed 30 April 2015].

[26] ARM, "Keil Tools by ARM," 2013. [Online]. Available: http://www.keil.com/arm/mdk.asp. [Accessed March 2015].

[27] Segger, "Segger: The Embedded Experts," 2015. [Online]. Available: https://www.segger.com/jlink-debug-probes.html. [Accessed March 2015].

[28] S. C. Mukhopadhyay, "Wearable Sensors for Human Activity Monitoring: A Review", *IEEE Sensors Journal*, vol. 15, no. 3, pp. 1321-1330, 2015

[29] Analog Devices, "Analog Devices," 2012. [Online]. Available: http://www.analog.com/media/en/technical-documentation/obsolete-data-sheets/ADMP401.pdf. [Accessed March 2015].

[30] Honeywell, "Farnell," 2015. [Online]. Available: http://sensing.honeywell.com/index.php?ci_id=49692. [Accessed March 2015].

[31] Texas Instruments, "LMT86/LMT86-Q1 SC70/TO-92/TO-126, Analog Temperature Sensors," May 2014. [Online]. Available: http://www.mouser.com/ds/2/405/snis169b-338024.pdf. [Accessed March 2015].

[32] Highcharts, "Highcharts: MAKE YOUR DATA COME ALIVE," 2015. [Online]. Available: http://www.highcharts.com/. [Accessed March 2015].

[33] Maxim Integrated, "Datasheets Maxim Integrated," January 2015. [Online]. Available: http://datasheets.maximintegrated.com/en/ds/DS1307.pdf. [Accessed 20 March 2015].

[34] E. Candes and M. Wakin, "An Introduction to Compressive Sampling," *IEEE Signal Processing Magazine,* vol. 21, no. 2, pp. 21 - 30, 2008.